Research Article

The use of titanium (IV) phosphate for metal removal from aqueous and alcoholic samples

Angelo R. F. Pipi[1,2] · Sidney Aquino Neto[3] · Priscila Fernanda Pereira Barbosa[2] · Devaney R. Do Carmo[2]

Abstract

Adsorption methods are widely employed for the removal of metals from aqueous medium, being an efficient and environmentally friendly technique for wastewater treatment. From the several adsorptive materials that are being employed by the specialized literature in removal processes, TiO_2 continues to be a wise choice. In this work, we have prepared a phosphate-modified TiO_2 (TiPh) and tested their adsorptive behavior toward different metallic species. TiPh synthesis was carried out from a titanium (IV) isopropoxide in aqueous phosphoric acid solution. The adsorption of Co^{+2}, Cu^{+2}, and Ni^{+2} in a TiPh matrix was investigated in different media: water, 42% ethanol aqueous solution, and pure ethanol. The kinetic assays results indicated that the adsorption equilibrium occurs after 10–40 min, being higher for alcoholic solutions. The higher capacity values were obtained in the 42% ethanol aqueous solution, in which N_f values of 9.1×10^{-4} mol g^{-1}, 5.9×10^{-4} mol g^{-1}, and 5.1×10^{-4} mol g^{-1} were obtained for Cu^{+2}, Co^{+2}, and Ni^{+2}, respectively.

Keywords Adsorption · Composite · Titanium phosphate · Metal ions · Langmuir adsorption model

1 Introduction

Transferring substances of particular interest from a liquid or gaseous phase to a solid material is a widespread concept that can be quite useful for analytical and environmental purposes [1]. The use of adsorption methodology is especially interesting for the removal of metallic species from aqueous solution once they are very hazardous to the environment [2]. Compared to other methods, adsorption processes show high efficiency with the convenience of easy operation, simplicity of design, and economic viability [3, 4]. In the past decades, various materials have been proposed for the achievement of efficient metal removal from different samples, focusing on both the treatment of wastewater and their quantification in industrial processes. Clays [5], chitosan [6], zeolites [7], different carbon materials [8], among others, are generally focused by research teams worldwide [3]. Another important material in the context of adsorption processes is the multifunctional titanium oxide (TiO_2) [9–11].

Titanium oxide is one of the most used amphoteric inorganic material in a wide variety of fields, such as analytical, electrochemistry, catalysis, environmental, and material science. TiO_2 can be obtained in many forms, such as sol–gels [12], nanoparticles [13], nanofibers [14], and nanotubes [15]. Thanks to their biocompatibility, stability, and environmental safety, titanium oxide has been applied in different manners such as solar energy conversion devices [16], photocatalysis [17], sensors [18], and photochromic devices [19]. In addition, because of their high ion exchange capacity, another promising aspect of this inorganic material is to act as an inorganic ion exchanger and sorbent, thus being useful for solid-phase extractions [20]. Considering the use of titanium oxide for adsorption

purposes, there are numerous works on the specialized literature, mainly for the removal of dyes and metallic species. In the first situation, dyes can be removed from aqueous solution directly via adsorption as well as by simultaneous adsorption and photocatalysis. Duta and Visa have shown the preparation of a fly-ash–TiO$_2$ composite for the simultaneous removal of two commercial dyes (bemacid red and bemacid blue) via adsorption and photocatalysis [21]. Considering the use of titanium oxide for metal removal, literature has covered a wide range of species. Yu and co-workers have shown the arsenite removal from aqueous solutions using γ-Fe$_2$O$_3$–TiO$_2$ magnetic nanoparticles with simultaneous photocatalytic oxidation and adsorption [22]. Nanostructured TiO$_2$ particles are also shown to be quite efficient for the removal of Cd(II) from wastewater in engineering practices [23]. TiO$_2$ nanotube is another form of the inorganic material that can be quite efficient for metal removal. Besides displaying a large BET surface area, such material can be employed for simultaneous hydrogen production and copper removal from water samples [24]. Another example is the synthesis of a nanocomposite material containing TiO$_2$/poly(acrylamide-styrene sodium sulfonate) for the removal of radioactive cesium, cobalt and europium ions [25].

Recently, different functionalized mesoporous conjugate nanomaterials were prepared for harmful organic compound adsorption and then used for diverse uses in metal ion removal and detection [26–34].

In previous investigation, we have prepared a titanium (IV) phosphate copper hexacyanoferrate composite from aqueous phosphoric acid and titanium (IV) isopropoxide (TiPh). The obtained hybrid material was fully characterized and displayed electrochemical stability with good reproducibility for the determination of N-acetylcysteine [35]. In this paper, the focus is placed on the synthesis of phosphate-modified TiO$_2$ and their adsorptive behavior toward different metallic species: Co^{+2}, Cu^{+2}, and Ni^{+2}. The goal was to evaluate the adsorption ability of this material in different media: water, 42% ethanol aqueous solution, and pure ethanol. Such evaluation is based on the fact that the presence of metals in many alcoholic beverages such as Brazilian Cachaça can be a significant parameter affecting their consumption, conservation, and their exportation [36].

2 Materials and methods

2.1 Chemicals

Titanium (IV) isopropoxide, phosphoric acid (85%), copper (II) chloride, cobalt (II) chloride, and nickel (II) chloride were of analytical grade (p.a Merck) and used without further

purification. All solutions were prepared with high-purity water from a Millipore Milli-Q system immediately before use.

2.2 Synthesis of phosphate-modified TiO$_2$ (TiPh)

Synthesis of the proposed adsorbent material was performed as described below. Titanium isopropoxide was employed as the precursor material for binding of the phosphate groups. Thirty-five milliliters of phosphoric acid was transferred to a 100-mL beaker along with 20 mL titanium (IV) isopropoxide and 10 mL water. After homogenization, the mixture was allowed to stand in the dark for 24 h. After that period, the formed solid phase was filtered and dried at room temperature for another day. The final powder material, named TiPh, was stored in a low-humidity environment glass recipient before use.

2.3 Metal adsorption studies using TiPh

The metal adsorption studies employing the modified titanium oxide were performed using a batchwise technique in thermostatic flasks at 25.0 ± 0.1 °C. The goal was to evaluate the adsorption ability of this material in different media: water, 42% ethanol aqueous solution, and pure ethanol. After equilibria, the samples were filtered to remove the adsorbent material followed by titration of each supernatant.

2.3.1 Determination of adsorption equilibrium time

In this step, adsorption experiments as a function time were performed using the modified titanium oxide and each metal species proposed in this work (Co^{+2}, Cu^{+2}, and Ni^{+2}). The protocol employed consisted of transferring 50 mg of the functionalized material to the thermostatic flasks, followed by addition of 5 mL aliquots of each metal solution (5.0 × 10^{-3} mol L^{-1}). The final volume in each flask was kept constant at 50 mL. The mixtures were shaken and collected at different intervals of time (5, 10, 20, 30, 40 and 50 min). After filtration, the nonadsorbed metal ions contained in the supernatant were quantified by titration. For determination of Cu^{+2} and Ni^{+2} ions, titrations were performed using 1.0 × 10^{-3} mol L^{-1} ethylenediaminetetraacetic acid (EDTA) solution as titrant at pH 10, which was maintained by an ammonia/ammonium chloride buffer. Murexide (ammonium purpurate) was employed as indicator in both titrations performed. For determination of Co^{+2} species, the same procedure using EDTA was employed; however, in this case, 1% hexamethylenetetramine and xylenol orange were employed as indicators.

2.3.2 Adsorbent capacity: adsorption curves

In this study, the same batchwise technique using thermostatic flasks at 25.0 ± 0.1 °C was employed. The amount of adsorbent was kept constant at 50 mg, and different aliquots (2.5, 5.0, 7.5, 10, 12.5, 15, 20, 25 and 30 mL) of the metal standard solutions (5×10^{-3} mol L^{-1}) were added in each vial, keeping the final volume in 50 mL. The solutions were stirred for the same time period previously described, followed by filtration. The nonadsorbed metal ions contained in the supernatant were quantified by titration through complexometric titrations as described in the previous item.

3 Results and discussion

3.1 Characterization of TipH

In a previous work [35], we report a complete characterization of TiPh and their use as an electrochemical sensor for the detection of n-acetylcysteine. Herein, we report its potential as an adsorbent composite for some transition metals such as copper (Cu^{+2}), cobalt (Co^{+2}) and nickel (Ni^{+2}) in different media.

3.2 Adsorption kinetic studies

Adsorption kinetic studies were carried out through typical adsorption curves, which are here expressed by the number of mol of solute adsorbed per unit of mass of adsorbent (N_f, mol g^{-1}) as a function of time (minutes). Adsorption kinetic assays were performed by evaluating the time needed for the metal species (Cu^{+2}, Co^{+2} and Ni^{+2}) to reach equilibrium with the phosphate-modified TiO$_2$ matrix at constant temperature (25 °C). For each metal evaluated, adsorption assays were performed in water, 42% ethanol aqueous solution, and pure ethanol. Such solutions aim to simulate real alcoholic samples such as alcoholic beverages and vehicle fuels. By varying the adsorption time from 5 to 50 min, we have observed that in aqueous medium the time required to reach the saturation of TiPh with Cu^{+2}, Co^{+2} and Ni^{+2} ions was about 30, 10 and 20 min, respectively, as shown in Fig. 1a. We must also mention that after approximately 20 min, a desorption process of Ni^{+2} species takes place, reaching a maximum around 30 min with a plateau formation after 40-min experiment. Considering the values obtained in a 42% ethanol aqueous solution, the adsorption times for the Cu^{+2}, Co^{+2}, and Ni^{+2} ions were of about 40, 20, and 30 min, respectively (Fig. 1b). For the test performed in a pure ethanol solution, saturation occurs only after 30 min for all the evaluated metal ions, as shown in Fig. 1c. Overall, the adsorption

kinetic studies showed that saturation time varies quite a lot (from 10 to 40 min) depending on the metallic specie as well as on the solution in which the experiment was performed. The terminal phosphate groups anchored in the TiPh structure strongly interact with the metal ions contained in the solution through electrostatic interactions, thus making the TiO$_2$ matrix quite efficient binding agent for the metallic cations. It is also noteworthy to mention that in all three evaluated solutions, the amount of solute adsorbed per unit of mass of adsorbent was always higher for Cu^{+2} species, followed by Co^{+2} and Ni^{+2} ions. Such behavior can be understood considering that the maximum adsorption of metallic species is intrinsically related to the pH of the solution. Literature has shown that Cu^{+2} ions should adsorb on solid material more easily in lower pH values, due to their partial hydrolysis that results in the formation of hydrolyzed species, and Ni^{+2} species should have higher maximum adsorption in alkaline media due to formation of both [NiOH]$^+$ and Ni(OH)$_2$ at these pHs [37]. Another TiO$_2$-based adsorption material has provided similar kinetic behavior [38].
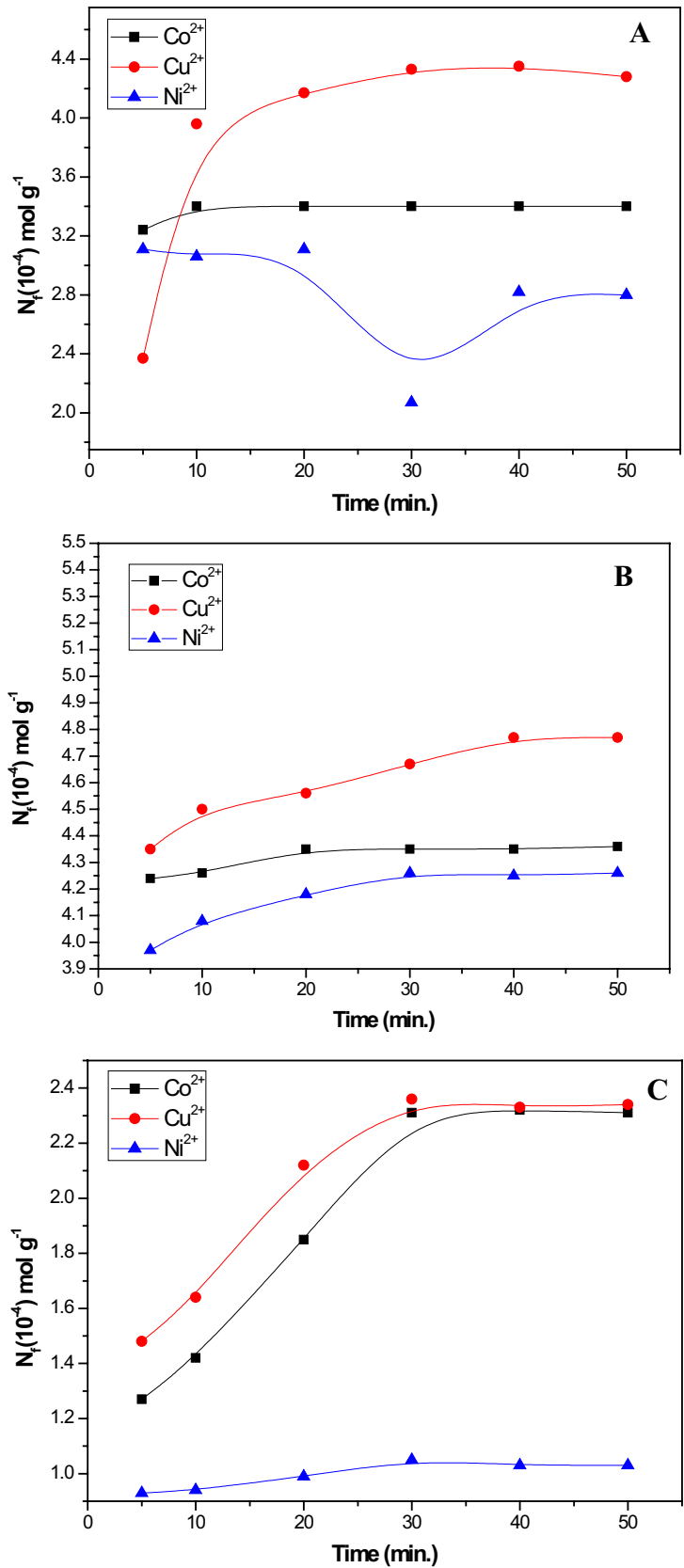
3.3 TiPh adsorption capacity

In order to evaluate the adsorption capacity of the modified TiO$_2$ for each metal ion, sorption isotherms were performed and expressed by the N_f/C ratio. The maximum amount of adsorbed metal ions (N_f^{max}), also named specific sorption capacity, is equal to the quantity of metal ions adsorbed when the concentration (C) tends to saturation. As stated in Eq. 1, the N_f values are calculated by the difference between the amount of each metallic ion added before equilibrium (N_b) and the amount of each metallic ions contained in the solution not adsorbed after equilibrium (N_s), divided by the adsorbent matrix mass (W) [39]:

$$N_f = \frac{(N_b - N_s)}{W} \tag{1}$$

In all the obtained isotherms, we have observed a similar adsorption behavior, where all the evaluated metal ions display low N_f and concentration at the beginning of the experiment. As the experiment proceeds, the concentration of the metal ion increases and the N_f value becomes independent until active site saturation occurs and N_f reaches a constant value. Figure 2 shows representative adsorption isotherms obtained with the TiPh adsorbent matrix for each metal evaluated. Adsorption capacity assays were performed in water, 42% ethanol aqueous solution, and pure ethanol. Considering the experiments performed in purified water (Fig. 2a), the results obtained with Cu^{+2} ions indicate a partial saturation of the TiPh active sites with 13×10^{-4} mol L^{-1} that still increase up to

Fig. 1 Adsorption kinetic assays performed with the metal species Cu^{+2}, Co^{+2}, and Ni^{+2} using the TiPh matrix at 25° C: **a** water, **b** 42% ethanol aqueous solution, **c** pure ethanol
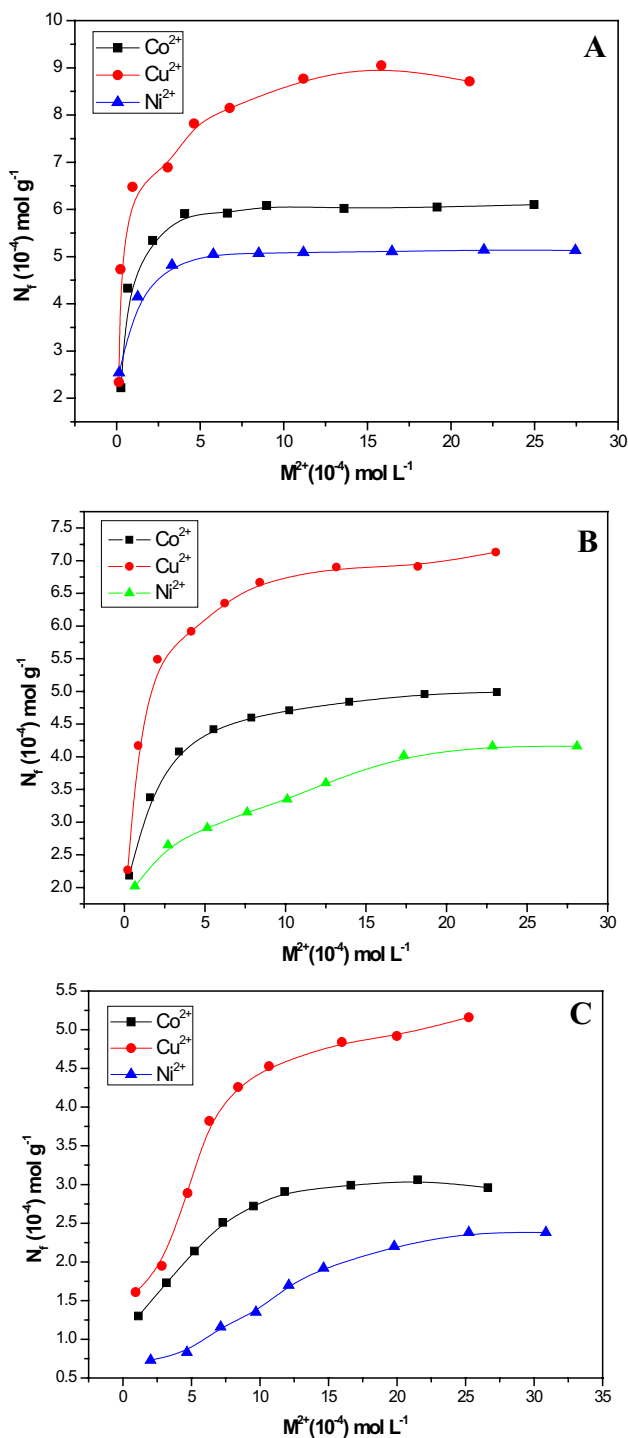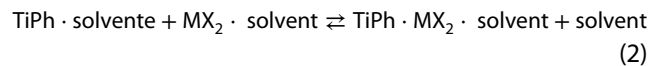
Fig. 2 Adsorption isotherms obtained with the TiPh matrix in different metal ions solutions (Cu^{+2}, Co^{+2}, and Ni^{+2}) at 25° C: **a** water, **b** 42% ethanol aqueous solution, **c** pure ethanol

23×10^{-4} mol L^{-1}, thus leading to an adsorptive capacity of N_f of 7.1×10^{-4} mol g^{-1}. As for the assay employing the other two metal ions, the isotherms indicate the saturation of TiPh active sites around 18.0×10^{-4} mol L^{-1} (N_f of

4.97×10^{-4} mol g^{-1}) and 22×10^{-4} mol L^{-1} (N_f of 4.1×10^{-4}) for Co^{+2} and Ni^{+2} ions, respectively. Again, as noticed in the previous section, the adsorption experiments indicate higher adsorption of Cu^{+2} ions in the TiPh structure, when compared to the other metallic species (Co^{+2} and Ni^{+2}).

The probable adsorption mechanism could be represented by Eq. 2:

$$TiPh \cdot solvente + MX_2 \cdot solvent \rightleftarrows TiPh \cdot MX_2 \cdot solvent + solvent \tag{2}$$

where $M = Cu^{+2}$, Co^{+2}, and Ni^{+2}

This matrix is chemically stable and easily reactivated, and does not leach and can be several times reused after percolation of 0.1 mol L^{-1} hydrochloric acid.

Figure 2b shows the isotherms obtained in the adsorption capacity experiments performed in a 42% ethanol aqueous solution containing Co^{+2}, or Cu^{+2}, or Ni^{+2} ions. Considering the results obtained with Cu^{+2} ions, we can observe a partial saturation of the TiPh active sites at 11×10^{-4} mol L^{-1}, followed by an increase in the adsorptive capacity, reaching values as high as 15×10^{-4} mol L^{-1} with a N_f of 9.1×10^{-4} mol g^{-1}. For Co^{+2} species, the obtained isotherm indicates the saturation of TiPh at 4.1×10^{-4} mol L^{-1} with a N_f of 5.9×10^{-4} mol g^{-1}. As for Ni^{+2} ions, saturation occurs at 5.8×10^{-4} mol L^{-1} with N_f of 5.1×10^{-4} mol g^{-1}. Finally, the adsorptive capacity results registered in pure ethanol are presented in Fig. 2 c. From the obtained Cu^{+2} isotherm, we could not observe TiPh active sites saturation in the concentration range evaluated. In fact, the maximum N_f recorded in Cu^{+2} solution was of 5.2×10^{-4} mol g^{-1}. Considering the assay performed in a solution containing Co^{+2} ions, saturation is observed at 16×10^{-4} mol L^{-1} with N_f of 3.0×10^{-4} mol g^{-1}. In the experiments performed in a pure ethanol solution containing Ni^{+2} species, TiPh active sites saturation is reached at 25×10^{-4} mol L^{-1} with a N_f of 2.4×10^{-4} mol g^{-1}.

Additionally, the TiPH is chemically stable and can be reused after 7 months of preparation (+ 60 cycles), simply by desorbing the metal ion washing the material (TiPHM where $M = Cu^{+2}$, Ni^{+2} and Co^{+2} with HCl 0.1 M and then with KOH 0.1 M to pH neutral (~ 7.0).

Comparing all six isotherms obtained in both alcoholic solutions tested, the absorption values achieved for Cu^{+2} species remain higher than both Co^{+2} and Ni^{+2}. Such behavior is justified by the previously mentioned pH effect, where Cu^{+2} species should adsorb more easily in TiPh at lower pH when compared to the other two metals due to the formation of Cu-hydrolyzed species. Higher adsorption values would be achieved for Ni species, for example, if such experiments were performed in more alkaline regions; however, considering the final goal of this work—preparing a material suitable to be employed for metal quantification and removal in beverage production

processes—such aspect was not focused on in this work. The adsorption behavior observed in all isotherms is understood considering that removal efficiencies of metal ions are affected by an increase in the ions concentration. At low concentrations, the adsorption process involves the higher energy surface sites, and as the metal species concentration increases, such sites are saturated and adsorption starts to happen on the lower energy surface sites, thus resulting in a decrease in the adsorption efficiency [40, 41].

3.4 Stability studies of the complexes formed on TiPh surface

The adsorption process of a solute to a solid matrix at constant temperature and volume involves a continuous competition between such species and the solvent molecules that are in contact with the adsorptive material surface. The complete sorption process can be obtained quantitatively from the sorption isotherms, in which the adsorbed amount data are determined after equilibrium. Assuming the formation of monolayers, the Langmuir equation (Eq. 3) can be applied to linearize the sorption isotherms and to estimate important parameters related to equilibrium:

$$\frac{C_s}{N_f} = \frac{C_s}{N_s} + \frac{1}{N_s k} \qquad (3)$$

In such equation, C_s represents the solution concentration at equilibrium (in mol L^{-1}); N_f is the adsorbent adsorption capacity (in mol g^{-1}); N_s is the maximum amount of solute adsorbed (in mol g^{-1}); and k is the measure of sorption intensity, which is related to the equilibrium constant. The linear regression from the plot of C_s/N_f as a function of C_s gives us $1/N_s$ and $1/(kN_s)$, which are the slope and the linear coefficients, respectively, allowing us to determine both k and N_s values [42]. Figure 3 shows the linearization isotherm plots of C_s/N_f as a function of C_s for each metal ion (Cu^{+2}, Ni^{+2}, and Co^{+2}) evaluated in adsorption assays in water, 42% ethanol aqueous solution, and pure ethanol.

Table 1 shows all the determined parameters after the adsorption tests employing the TiPh matrix in each solution containing Cu^{+2}, or Ni^{+2}, or Co^{+2}. The N_f maximum values are also presented for comparison purposes.

According to the Langmuir model, N_f values approach N_s at the surface saturation point. From the data presented in Table 1, we have observed that both N_f and N_s values determined in all the metallic solutions are quite close to the ones determined for each solvent studied, thus being in agreement with the Langmuir model. In particular, the absorption experiment with Ni^{+2} ions performed in pure ethanol showed some discrepancy
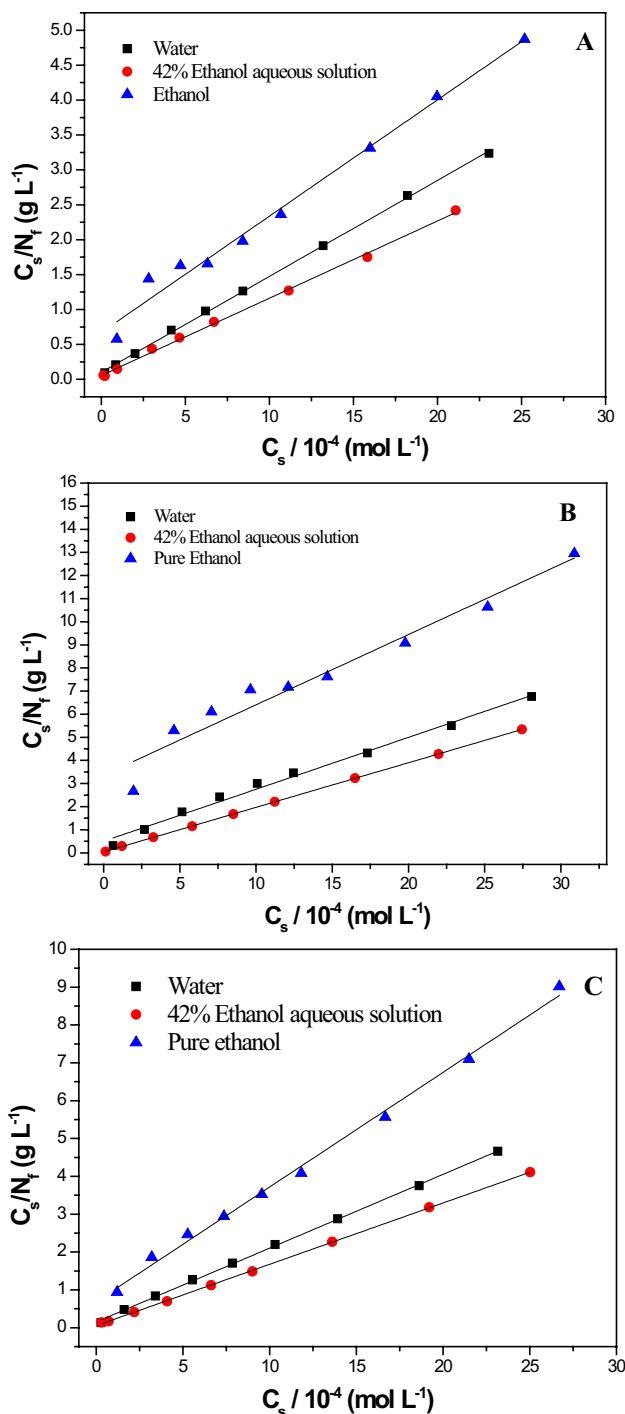

Fig. 3 Linearization isotherms plots of C_s/N_f as a function of C_s for each metal ion evaluated in adsorption assays. **a** Cu^{+2}. **b** Ni^{+2}, **c** Co^{+2}. Adsorption assays were performed in water, 42% ethanol aqueous solution, and pure ethanol

between the N_f and N_s values, which is probably related to the low correlation coefficient value obtained in this case or even to possible nonsaturation of the matrix surface in the concentration range studied and evaluated.

Table 1 k and N_s values determined by linear regression from the plot of C_s/N_f as a function of C_s after the adsorption assays in water, 42% ethanol aqueous solution, and pure ethanol with Cu^{+2}, Ni^{+2}, and Co^{+2}

Metal adsorbed	Solution	$N_f^{max}\,10^4$ (mol g^{-1})	$N_s\,10^4$ (mol g^{-1})	$k\,10^{-3}$ (L mol^{-1})	R
Cu^{+2}	Water	7.1	7.3	10	0.999
	42% ethanol	9.1	9.0	18	0.998
	Pure ethanol	5.2	6.0	1.5	0.984
Ni^{+2}	Water	4.2	4.5	2.0	0.991
	42% ethanol	5.2	5.2	25	0.999
	Pure ethanol	2.4	3.3	0.3	0.949
Co^{+2}	Water	5.0	5.1	6.6	0.999
	42% ethanol	6.1	6.2	19	0.999
	Pure ethanol	3.0	3.3	1.5	0.995

Table 2 Comparison of adsorption capacity from this modified phosphate with that of different types of sorbents reported in references

Metal	Adsorbent material	Adsorption capacity (mg/g)	References
Copper	Biochar	5.0	[51]
Copper	Porous ceramsite	9.42	[52]
Copper	Pomegranate peel (PGP)	30.12	[53]
Copper	PEI-modified mass	48.60	[54]
Copper	Modified phosphate	57.83	This work
Cobalt	DTPA chitosan	2.35	[55]
Cobalt	Modified chitosan	2.78	[56]
Cobalt	DTPA silica gel	8.56	[55]
Cobalt	Palygorskite	8.88	[57]
Cobalt	Modified phosphate	34.76	This work
Nickel	Hybrid membrane	10.29	[58]
Nickel	Modified brown algae	11.67	[59]
Nickel	Clay adsorbents	15.70	[60]
Nickel	Imprinted polymer	19.86	[61]
Nickel	Modified phosphate	29.93	This work

Finally, the isotherms linearization allowed us to calculate the sorption intensity of each complex, represented by the constant k. Based on the high values obtained, the complexes formed at the surface of the adsorbent should be thermodynamically stable. In summary, the obtained data are quite satisfactory compared to recent literature displaying a high level of applicability potential [43–50]. For comparison, Table 2 lists the maximum adsorption capacity obtained from this material with that reported in the literature. Clearly, the adsorption capacity of copper(II), cobalt(II) and nickel(II) ions was satisfactory.

4 Conclusions

The synthesis of phosphate-modified TiO_2 was achieved from their isopropoxide form in an efficient one-pot methodology. The adsorption kinetic assays performed in different solutions containing Cu^{+2}, Co^{+2}, or Ni^{+2} indicated that the adsorption equilibrium between the metal species and the TiPh matrix occurs after 10–40 min, being higher in the alcoholic solutions. The amount of metal species adsorbed onto the TiPh surface followed the sequence $Cu^{+2} > Co^{+2} > Ni^{+2}$, which is mainly related to the solution pH that, once Cu^{+2} ions should adsorb more easily in the TiPh structure at lower pH when compared to the other two metals due to the formation of Cu-hydrolyzed species. In the adsorption capacity experiments, the obtained isotherms indicated similar adsorption behavior for all the metal species evaluated, with higher capacity values being achieved in the 42% ethanol aqueous solution. In such situation, N_f values of 9.1×10^{-4} mol g^{-1}, 5.9×10^{-4} mol g^{-1} and 5.1×10^{-4} mol g^{-1} were obtained for Cu^{+2}, Co^{+2} and Ni^{+2}, respectively. Finally, linearization isotherms showed that all the adsorption experiments performed follow the Langmuir model. Moreover, based on the high value of k obtained, the complexes formed at the surface of the adsorbent should be thermodynamically stable. Overall, from all the adsorption experiments in TiPh performed for Co^{+2}, Cu^{+2} and Ni^{+2} in different media, we observed that such material displays high potential applicability for metal quantification and removal, especially for alcoholic solutions such as beverages and vehicle fuels that must have their quantity of metal continuously evaluated during the production process due to the high environmental control that is necessary in such samples.

Compliance with ethical standards

Conflict of interest The author(s) declare that they have no competing interests.

References

1. Dąbrowski A (2001) Adsorption—from theory to practice. Adv Colloid Interface Sci 93:135–224. https://doi.org/10.1016/S0001-8686(00)00082-8
2. Fu FL, Wang Q (2011) Removal of heavy metal ions from wastewaters: a review. J Environ Manag 92:407–418. https://doi.org/10.1016/j.jenvman.2010.11.011

3. Babel S, Kurniawan TA (2003) Low-cost adsorbents for heavy metals uptake from contaminated water: a review. J Hazard Mater 97:219–243. https://doi.org/10.1016/S0304-3894(02)00263-7

4. Bailey SE, Olin TJ, Bricka RM, Adrian DD (1999) A review of potentially low-cost sorbents for heavy metals. Water Res 33:2469–2479. https://doi.org/10.1016/S0043-1354(98)00475-8

5. Celis R, Hermosin MC, Cornejo J (2000) Heavy metal adsorption by functionalized clays. Environ Sci Technol 34:4593–4599. https://doi.org/10.1021/es000013c

6. Ngah WSW, Teong LC, Hanafia M (2011) Adsorption of dyes and heavy metal ions by Chitosan composites: a review. Carbohydr Polym 83:1446–1456. https://doi.org/10.1016/j.carbpol.2010.11.004

7. Motsi T, Rowson NA, Simmons MJH (2009) Adsorption of heavy metals from acid mine drainage by natural zeolite. Int J Miner Process 92:42–48. https://doi.org/10.1016/j.minpro.2009.02.005

8. Kobya M, Demirbas E, Senturk E, Ince M (2005) Adsorption of heavy metal ions from aqueous solutions by activated carbon prepared from apricot stone. Biores Technol 96:1518–1521. https://doi.org/10.1016/j.biortech.2004.12.005

9. Kitano M, Matsuoka M, Ueshima M, Anpo M (2007) Recent developments in titanium oxide-based photocatalysts. Appl Catal A 325:1–14. https://doi.org/10.1016/j.apcata.2007.03.013

10. Sekino T (2010) Synthesis and applications of titanium oxide nanotubes, in inorganic and metallic nanotubular materials: recent technologies and applications. Springer, Berlin

11. Rahimi N, Pax RA, Gray EM (2016) Review of functional titanium oxides. I: TiO_2 and its modifications. Prog Solid State Chem 44:86–105. https://doi.org/10.1016/j.progsolidstchem.2016.07.002

12. Wang XD, Shi F, Gao X, Fan C, Huang W, Feng X (2013) A sol-gel dip/spin coating method to prepare titanium oxide films. Thin Solid Films 548:34–39. https://doi.org/10.1016/j.tsf.2013.08.056

13. El-Deen S, Zhang FS (2016) Immobilisation of TiO_2-nanoparticles on sewage sludge and their adsorption for cadmium removal from aqueous solutions. J Exp Nanosci 11:239–258. https://doi.org/10.1080/17458080.2015.1047419

14. Chen DZ, Liu C, Chen S, Shen W, Luo X, Guo L (2016) Controlled synthesis of recyclable, porous FMO/C@TiO_2 core-shell nanofibers with high adsorption and photocatalysis properties for the efficient treatment of dye wastewater. ChemPlusChem 81:282. https://doi.org/10.1002/cplu.201500534

15. Liu W, Ni JR, Yin XC (2014) Synergy of photocatalysis and adsorption for simultaneous removal of Cr(VI) and Cr(III) with TiO_2 and titanate nanotubes. Water Res 53:12–25

16. Hochbaum AI, Yang PD (2010) Semiconductor nanowires for energy conversion. Chem Rev 110:527–546. https://doi.org/10.1021/cr900075v

17. Nakata K, Fujishima A (2012) TiO_2 photocatalysis: design and applications. J Photochem Photobiol C 13:169–189. https://doi.org/10.1016/j.jphotochemrev.2012.06.001

18. Li XG, Li X, Wang J, Lin S (2015) Highly sensitive and selective room-temperature formaldehyde sensors using hollow TiO_2 microspheres. Sens Actuators B Chem 219:158–163. https://doi.org/10.1016/j.snb.2015.05.031

19. Djaoued Y, Balaji S, Beaudoin N (2013) Sol-gel synthesis of mesoporous WO_3–TiO_2 composite thin films for photochromic devices. J Sol Gel Sci Technol 65:374–383. https://doi.org/10.1007/s10971-013-3218-z

20. Shen Q, Yang M, Li L, Cheung HY (2014) Graphene/TiO_2 nanocomposite based solid-phase extraction and matrix-assisted laser desorption/ionization time-of-flight mass spectrometry for lipidomic profiling of avocado (Persea americana Mill.). Anal Chim Acta 852:153–161. https://doi.org/10.1016/j.aca.2014.09.022

21. Duta A, Visa M (2015) Simultaneous removal of two industrial dyes by adsorption and photocatalysis on a fly-ash–TiO_2 composite. J Photochem Photobiol A 306:21–30. https://doi.org/10.1016/j.jphotochem.2015.03.007

22. Yu L, Peng X, Ni F, Li J, Wang D, Luan Z (2013) Arsenite removal from aqueous solutions by γ-Fe_2O_3–TiO_2 magnetic nanoparticles through simultaneous photocatalytic oxidation and adsorption. J Hazard Mater 246–247:10–17. https://doi.org/10.1016/j.jhazmat.2012.12.007

23. Zha R, Nadimicherla R, Guo X (2014) Cadmium removal in waste water by nanostructured TiO_2 particles. J Mater Chem A 2:13932–13941. https://doi.org/10.1039/C4TA02106A

24. Xu S, Ng J, Du AJ, Liu J, Sun DD (2011) Highly efficient TiO_2 nanotube photocatalyst for simultaneous hydrogen production and copper removal from water. Int J Hydrogen Energy 36:6538–6548. https://doi.org/10.1155/2012/843042

25. Borai EH, Breky MME, Sayed MS, Abo-Aly MM (2015) Synthesis, characterization and application of titanium oxide nanocomposites for removal of radioactive cesium, cobalt and europium ions. J Colloid Interface Sci 450:17–25. https://doi.org/10.1016/j.jcis.2015.02.0620021-9797

26. Awual MdR, Miyazaki Y, Taguchi T, Shiwaku H, Yaita T (2016) Encapsulation of cesium from contaminated water with highly selective facial organic–inorganic mesoporous hybrid adsorbent. Chem Eng J 291:128–137. https://doi.org/10.1016/j.cej.2016.01.109

27. Awual MdR (2016) Solid phase sensitive palladium(II) ions detection and recovery using ligand based efficient conjugate nanomaterials. Chem Eng J 300:264–272. https://doi.org/10.1016/j.cej.2016.04.071

28. Awual MR, Hasan MM, Khaleque MA, Sheikh MC (2016) Treatment of copper(II) containing wastewater by a newly developed ligand based facial conjugate materials. Chem Eng J 288:368–376. https://doi.org/10.1016/j.cej.2015.11.108

29. Shahat A, Awual MdR, Naushad Mu (2015) Functional ligand anchored nanomaterial based facial adsorbent for cobalt(II) detection and removal from water samples. Chem Eng J 271:155–163. https://doi.org/10.1016/j.cej.2015.02.097

30. Awual MdR, Alharthi N, Hasan MdM, Karim MR, Islam A, Znad H, Hossain MA, Halim MdE, Rahman MM, Khaleque MA (2017) Inorganic-organic based novel nano-conjugate material for effective cobalt(II) ions capturing from wastewater. Chem Eng J 324:130–139. https://doi.org/10.1016/j.cej.2017.05.026

31. Awual MR, Alharthi NH, Okamoto Y, Karim MR, Halim MdE, Hasan MdM, Rahman MM, Islam MM, Khaleque MA, Sheikh MC (2017) Ligand field effect for Dysprosium(III) and Lutetium(III) adsorption and EXAFS coordination with novel composite nanomaterials. Chem Eng J 320:427–435. https://doi.org/10.1016/j.cej.2017.03.075

32. Awual MR, Hasan MM, Eldesoky G, Khaleque MA, Rahman MM, Naushad M (2016) Facile mercury detection and removal from aqueous media involving ligand impregnated conjugate nanomaterials. Chem Eng J 290:243–251. https://doi.org/10.1016/j.cej.2016.01.038

33. Awual MR, Hasan MM, Shahat A, Naushad M, Shiwaku H, Yaita T (2015) Investigation of ligand immobilized nano-composite adsorbent for efficient cerium(III) detection and recovery. Chem Eng J 265:210–218. https://doi.org/10.1016/j.cej.2014.12.052

34. Awuala MdR, Yaita T, Taguchi T, Shiwaku H, Suzuki S, Okamoto Y (2014) Selective cesium removal from radioactive liquid waste by crownether immobilized new class conjugate adsorbent. J Hazard Mater 278:227–235. https://doi.org/10.1016/j.jhazmat.2014.06.01135

35. Pipi ARF, do Carmo DR (2011) Voltammetric studies of titanium (IV) phosphate modified with copper hexacyanoferrate and electroanalytical determination of N-acetylcysteine. J

Appl Electrochem 41:787–793. https://doi.org/10.1007/s10800-011-0296-x

36. Ibanez JG, Carreon-Alvarez A, Barcena-Soto M, Casillas N (2008) Metals in alcoholic beverages: a review of sources, effects, concentrations, removal, speciation, and analysis. J Food Compos Anal 21:672–683. https://doi.org/10.1016/j.jfca.2008.06.005

37. Kadirvelu K, Faur-Brasquet C, Cloirec PL (2000) Removal of Cu(II), Pb(II), and Ni(II) by adsorption onto activated carbon cloths. Langmuir 16:8404–8409. https://doi.org/10.1021/la0004810

38. Engates KE, Shipley HJ (2011) Adsorption of Pb, Cd, Cu, Zn, and Ni to titanium dioxide nanoparticles: effect of particle size, solid concentration, and exhaustion. Environ Sci Pollut Res 18:386–395. https://doi.org/10.1007/s11356-010-0382-3

39. Dias Filho NL (1998) Adsorption of copper(II) and cobalt(II) complexes on a silica gel surface chemically modified with 3-amino-1,2,4-triazole. Colloids Surf A Physicochem Eng Asp 144:219–227. https://doi.org/10.1016/S0927-7757(98)00569-X

40. Mark RM, Brian ER (1993) Modeling Cd adsorption in single and binary adsorbent (PAC) systems. J Environ Eng 119:332–348. https://doi.org/10.1061/(ASCE)0733-9372

41. Marzal P, Seco A, Gabaldón C, Ferrer J (1996) Cadmium and zinc adsorption onto activated carbon: influence of temperature, pH and metal/carbon ratio. J Chem Technol Biotechnol 66:279–285. https://doi.org/10.1002/(SICI)1097-4660

42. Rosa AH, Goveia D, Bellin IC, Lessa SS, Filho NLD (2006) New analytical procedure based on a cellulose bag and ionic exchanger with p-aminobenzoic acid groups for differentiation of labile and inert metal species in aquatic systems. Anal Bioanal Chem 386:2153–2160

43. Awual MdR (2019) Novel conjugated hybrid material for efficient lead(II) capturing from contaminated wastewater. Mater Sci Eng C 101:686–695. https://doi.org/10.1016/j.msec.2019.04.015

44. Awual MdR (2019) Innovative composite material for efficient and highly selective Pb(II) ion capturing from wastewater. J Mol Liq 284:502–510. https://doi.org/10.1016/j.molliq.2019.03.157

45. Awual MdR, Yaita T, Suzuki S, Shiwaku H (2015) Ultimate selenium(IV) monitoring and removal from water using a new class of organic ligand based composite adsorbent. J Hazard Mater 291:111–119. https://doi.org/10.1016/j.jhazmat.2015.02.066

46. Awuala MdR, Hasanb MdM (2015) Colorimetric detection and removal of copper(II) ions from wastewater samples using tailor-made composite adsorbent. J Sens Actuators B 206:692–700. https://doi.org/10.1016/j.snb.2014.09.086

47. Awual MdR, Yaita T, Shiwaku H (2013) Design a novel optical adsorbent for simultaneous ultra-trace cerium(III) detection, sorption and recovery. Chem Eng J 228:327–333. https://doi.org/10.1016/j.cej.2013.05.010

48. Awual MdR, Hasan MdM, Znad H (2015) Organic–inorganic based nano-conjugate adsorbent for selective palladium(II) detection, separation and recovery. Chem Eng J 259:611–619. https://doi.org/10.1016/j.cej.2014.08.028

49. Awual MdR, Yaita T, Shiwaku H, Suzuki S (2015) A sensitive ligand embedded nano-conjugate adsorbent for effective cobalt(II) ions capturing from contaminated water. Chem Eng J 276:1–10. https://doi.org/10.1016/j.cej.2015.04.058

50. Awual MdR, Asiri AM, Rahman MM, Alharthic N (2019) Assessment of enhanced nitrite removal and monitoring using Ligand modified stable conjugate materials. Chem Eng J 363:64–72. https://doi.org/10.1016/j.cej.2019.01.125

51. Hoslett J, Ghazal H, Ahmad D, Jouhara H (2019) Removal of copper ions from aqueous solution using low temperature biochar derived from the pyrolysis of municipal solid waste. Sci Total Environ 673:777–789. https://doi.org/10.1016/j.scitotenv.2019.04.085

52. Qing-xiu J, Yun-yan W, Li-yuan C, Chong-jian T, Xiao-dong H, Huan G, Wei W, Wei Y (2018) Adsorption of copper ions on porous ceramsite prepared by diatomite and tungsten residue. T Nonferrous Met Soc 28:1053–1060. https://doi.org/10.1016/S1003-6326(18)64731-4.53

53. Ben-Ali S, Jaouali I, Souissi-Najar S, Ouederni A (2017) Characterization and adsorption capacity of raw pomegranate peel biosorbent for copper removal. J Clean Prod 142:3809–3821. https://doi.org/10.1016/j.jclepro.2016.10.081

54. Jiajia D, Yangyang D, Rusheng D, Yu S, Shusheng Z, Runping H (2019) Adsorption of copper ion from solution by polyethylenimine modified wheat straw. Bioresour Technol Rep 6:96–102. https://doi.org/10.1016/j.biteb.2019.02.011

55. Repo E, Malinen L, Koivula R, Harjula R, Sillanpää M (2011) Capture of Co(II) from its aqueous EDTA-chelate by DTPA-modified silica gel and chitosan. J Hazard Mater 187:122–132. https://doi.org/10.1016/j.jhazmat.2010.12.113

56. Zhuang S, Yin Y, Wang J (2018) Removal of cobalt ions from aqueous solution using chitosan grafted with maleic acid by gamma radiation. Nuclear Eng Technol 50:211–215. https://doi.org/10.1016/j.net.2017.11.007

57. He M, Zhu Y, Yang Y, Han B, Zhang Y (2011) Adsorption of cobalt(II) ions from aqueous solutions by palygorskite. Appl Clay Sci 54:292–296. https://doi.org/10.1016/j.clay.2011.09.013

58. Irani M, Keshtkar AR, Mousavian MA (2011) Removal of Cd(II) and Ni(II) from aqueous solution by PVA/TEOS/TMPTMS hybrid membrane. Chem Engin J 175:251–259. https://doi.org/10.1016/j.cej.2011.09.102

59. Mehdi M, Rahmati M, Rabbani P, Abdolali A, Keshtkar AR (2011) Kinetics and equilibrium studies on biosorption of cadmium, lead, and nickel ions from aqueous solutions by intact and chemically modified brown algae. J Hazard Mater 185:401–407. https://doi.org/10.1016/j.jhazmat.2010.09.047

60. Gupta SS, Bhattacharyya KG (2006) Adsorption of Ni(II) on clays. J Colloid Interface Sci 295:21–32. https://doi.org/10.1016/j.jcis.2005.07.073

61. He J, Shang H, Zhang X, Sun X (2018) Synthesis and application of ion imprinting polymer coated magnetic multi-walled carbon nanotubes for selective adsorption of nickel ion. Appl Surf Sci 428:110–117. https://doi.org/10.1016/j.apsusc.2017.09.123